Azam Shafieenezhadet al. 2019, 7:6
ISSN (Online): 2348-4098
ISSN (Print): 2395-4752

International Journal of Science, Engineering and Technology

An Open Access Journal

Excited state emission of three state lasing semiconductor Quantum dot lasers for biospectroscopy applications

[1]Azam Shafieenezhad [2]Saeed Yazdani [3]Esfandiar Rajaei
Indiana University Purdue University Indianapolis, Indianapolis, IN, USA

***Abstract*- We study the excited states (ES) of semiconductor lasers by considering InGaAs/GaAs quantum dot (QD) laser rate equations which are solved numerically. For different values of compression gain, dynamics of a semiconductor QD laser for enhancing its small signal and large signal modulation is studied. We also have calculated turn on delay and output power as a function of compression gain. It is shown that for different values of compression gain the laser is unresponsive and turns on delay remains constant. Also, by increasing the value of compression gain output power increases. These special characteristics of ES of In GaAs/GaAs QD lasers make them a good candidate for use in bio imaging detectors and bio spectroscopy purposes.**

***Keywords*-Compression gain, Output power, Quantum dot laser, Large signal response.**

I. INTRODUCTION

The wide bandwidth and large exciton binding energy of InGaAs/GaAs QD lasers may generate new applications in bio-imaging after careful surface modifications. Facilitating lasers with an increased modal and spectral gain [1-6] in recent years, the performance of long wavelength quantum dot (QD) materials has improved significantly. This improvement has an undeniable effect on the properties of directly modulated lasers,leading to new record values in digital modulation rates obtained in the 1.3 µm GaAs based [3].

QD lasers are an attractive choice for next generation telecommunication networks, because ofproperties such as low threshold current [7-9], temperature insensitivity [10], high bandwidth [11,13] and low chirp [13,14]. Besides telecommunication application, the wavelength of this QD laser along with other characteristics such as small turn on delay and low threshold intensity are well suited for biomedical imaging.

In order to enhance the modulation properties and achieve the best responsemanypossible solutions have been explored including injection-locking [15], tunnelling injection [16] or p-doping [17]. However, for standard QD lasers the modulation bandwidth is still much lowerthan the best values reported for quantum well (QW) lasers [18]. Therefore, it is essential to examine the origin of such a limitation. It is obvious that the modulation bandwidth is highly dependent on the resonance frequency. The resonance frequency is restricted by the maximum modal gain and by gain compression effects [19].

In this paper, we theoretically probe the intensity modulation characteristics of InGaAs/GaAs QD lasers with a three state lasing model including a direct relaxation channel. A new analytical modulation transfer function is derived through a small-signal analysis of the differential rate equations. The analysis provides a proper understanding of theimpacts of the compression gain on different properties of ES emission which makes this state candidate for designing new high-tech and low cost biomedical imaging apparatuses.

II. MATHEMATICAL MODELING

In this section, three levels rate equation model with analytical forms which allow quantitative analyses ofexperimental data are derived. Also, a numerical model is used to study carrier dynamics in energylevels of an InGaAs/GaAs QD system [7]. In our model, there are four discrete energy levels, i.e.,

© 2019Azam Shafieenezhadet al. This is an Open Access article distributed under the terms of the Creative Commons Attribution License (http://creativecommons.org/licenses/by/4.0), which permits unrestricted use, distribution, and reproduction in any medium, provided the original work is properly credited.

wetting layer (WL), CS, GS, and ES of each group of QD. A few similar assumptions are made in the simulation model. Firstly, distribution of QDs is random in each layer of the device structure. Secondly, there is no correlation among different dot layers, thus simplifying the calculation. Thirdly, all carriers in each group of QD ensembles have the same relaxation and recombination rates. Lastly, carrier emission from higher dimensional confinement to lower confinement does not change with temperature but depends dominantly on the probability of carrier population. Besides that, a series of longitudinal cavity photon modes are taken into account over the inter-band transition energy of QDs to describe the interaction between the dots with different resonant energies and generated photons. Carrier thermal emission is assumed to occur among three energy levels in QD ensembles and between CS and WL.

The details of carrier population relaxation and reemission dynamics are schematically illustrated in Fig. 1. To properly describe the lasing characteristics of our 1.33μm quantum dot lasers which emit at ground states of the quantum dot, we consider three states; one for the photon at the lasing emission, one for the carrier in the ground state of the quantum dots, and the other for the carrier at the non-lasing states such as the excited states, upper continuum state and the wetting layer states[8].

$$\frac{dN_w}{dt} = \frac{\eta_i I}{e} - \frac{N_w}{T_{wr}} - \frac{N_w}{T_{wu_\circ}}(1-P_u) - \frac{N_e}{T_e} + \frac{N_u}{T_{uw}} - \frac{N_w}{T_r} \tag{1}$$

$$\begin{aligned}\frac{dN_u}{dt} &= \frac{N_w}{T_{wu\circ}}(1-P_u) + \frac{N_g}{T_{gu}}(1-P_u) \\ &- \frac{N_u}{T_{ue\circ}}(1-P_e) - \frac{N_u}{T_{uw}} - \frac{N_u}{T_e} - \frac{N_u}{T_r} \\ &- \Gamma v_g K_u (2P_u - 1) \times \left(\frac{S_u}{1+\epsilon_{us} S_u} \right)\end{aligned} \tag{2}$$

$$\begin{aligned}\frac{dN_e}{dt} &= \frac{N_u}{T_{ue\circ}}(1-P_e) + \frac{N_g}{T_{ge}}(1-P_e) \\ &- \frac{N_e}{T_{eu}}(1-P_u) - \frac{N_e}{T_{eg\circ}}(1-P_g) \\ &- \frac{N_e}{T_e} - \frac{N_e}{T_r} - \Gamma\ v_g\ K_e(2P_e - 1) \times \left(\frac{S_e}{1+\epsilon_{es} S_e} \right)\end{aligned} \tag{3}$$

$$\begin{aligned}\frac{dN_g}{dt} &= \frac{N_u}{T_{ug\circ}}(1-P_g) + \frac{N_e}{T_{eg\circ}}(1-P_g) \\ &- \frac{N_g}{T_{gu}}(1-P_u) - \frac{N_g}{T_{ge}}(1-P_e) \\ &- \frac{N_g}{T_e} - \frac{N_g}{T_r} - \Gamma\ v_g\ K_g(2P_g - 1) \times \left(\frac{S_g}{1+\epsilon_{gs} S_g} \right)\end{aligned} \tag{4}$$

$$\frac{dS_u}{dt} = \Gamma\ v_g\ K_u(2P_u - 1)\left(\frac{S_u}{1+\epsilon_{us} S_u}\right) + \frac{\beta N_u}{T_{sp}} - \frac{S_u}{T_P} \tag{5}$$

$$\frac{dS_e}{dt} = \Gamma\ v_g\ K_e(2P_e - 1)\left(\frac{S_e}{1+\epsilon_{es} S_e}\right) + \frac{\beta N_e}{T_{sp}} - \frac{S_e}{T_P} \tag{6}$$

$$\frac{dS_g}{dt} = \Gamma\ v_g\ K_g(2P_g - 1)\left(\frac{S_g}{1+\epsilon_{gs} S_g}\right) + \frac{\beta N_g}{T_{sp}} - \frac{S_g}{T_P} \tag{7}$$

The parameters of N_w, N_u, N_e, N_g refer to total carrier population of the wetting layer, carrier population of the upper continuum state (CS), exited state (ES) and ground state (GS), respectively. Also S_u, S_e, S_g refer to the photon density of CS, ES and GS, respectively and ϵ_{us}, ϵ_{es}, and ϵ_{gs} are gain compressions. For the above rate equations, optical gain for CS, ES and GS states can be wrote as follows:

$$g_{cs} = \frac{2\pi e^2 \hbar D_u}{c n_r \varepsilon_\circ m_\circ^2 v_d} \frac{|P_{cv}|^2}{E_u} \frac{\xi}{\Gamma_\circ}(2P_u - 1) = K_u(2P_u - 1) \tag{8}$$

$$g_{es} = \frac{2\pi e^2 \hbar D_e}{c n_r \varepsilon_\circ m_\circ^2 v_d} \frac{|P_{cv}|^2}{E_e} \frac{\xi}{\Gamma_\circ}(2P_e - 1) = K_e(2P_e - 1) \tag{9}$$

$$g_{gs} = \frac{2\pi e^2 \hbar D_g}{c n_r \varepsilon_\circ m_\circ^2 v_d} \frac{|P_{cv}|^2}{E_g} \frac{\xi}{\Gamma_\circ}(2P_g - 1) = K_g(2P_g - 1) \tag{10}$$

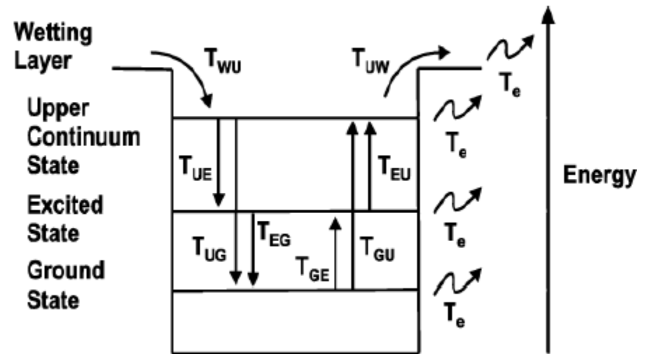

Figure1.Schematic of the energy band diagram that indicates the four different energy levels of wetting layer, upper continuum state, excited state and ground state of each group of QD ensemble. The inclusion of carrier capture and escape lifetime from the various states are shown[7].

P_u, P_e, P_g are occupation probabilities of continuum states (CS), ES and ground state(GS), respectively.

$$P_u = \frac{N_u}{2D_u N_D} \tag{11}$$

$$P_e = \frac{N_e}{2D_e N_D} \tag{12}$$

$$P_g = \frac{N_g}{2D_g N_D} \tag{13}$$

The perturbation step must be within the linear region. We have considered typical SAQDL material and typical geometrical parameters such as those given in Table 1 [20-22].

III. RESULTS

In this section, numerical results are presented. Photon density was calculated for ES and plotted for various values of compression gain (Fig 2.). Turn on delay was constant and photon density after relaxation oscillations decreased slightly. Considering these four same values for compression gain, we calculated photon density as a function of time for ES. It is not difficult to infer that by increasing compression gain, relaxation oscillations will decrease, turn on delay will be constant and photon density after passing 0.8 ns will be constant as well.

In Fig.3 we show photon density as a function of both time and digital current for ES in absence of compression gain. Clearly, without compression gain relaxation oscillations will appear and current will increase dramatically when we have lasing from ES. Next, we calculated photon density in the presence of compression gain. From Fig.4, it is clear that in the presence of compression gain the relaxation oscillations reduce dramatically. It can also be seen that relaxation oscillation for ES dramatically decreases. Current required to begin lasing in ES increases since to start lasing from higher levels there is a need to increase bias current in active region.

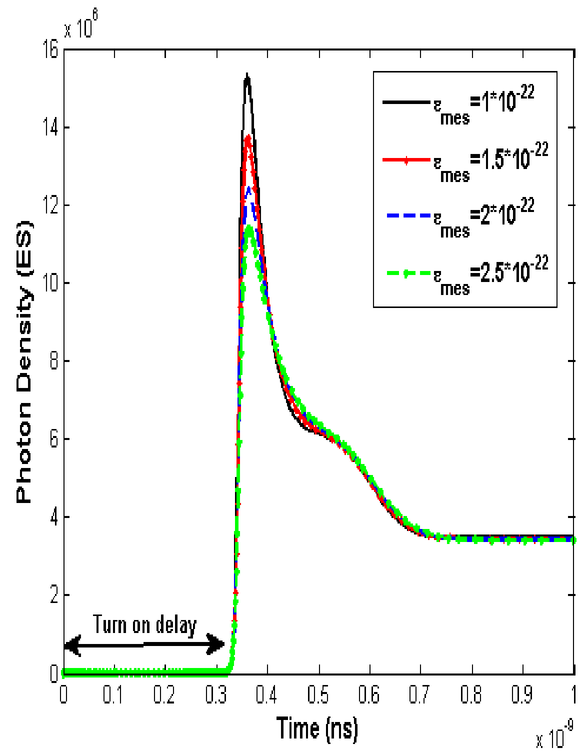

Figure 2: Photon density ES as a function of time for three values of compression gain.

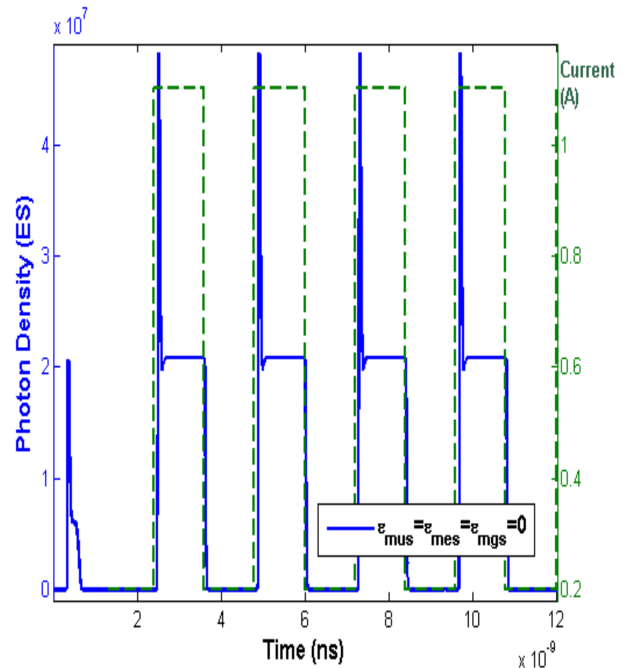

Figure 3 Large signal diagram ofphoton density as a function of time and digital current without compression gain for ES.

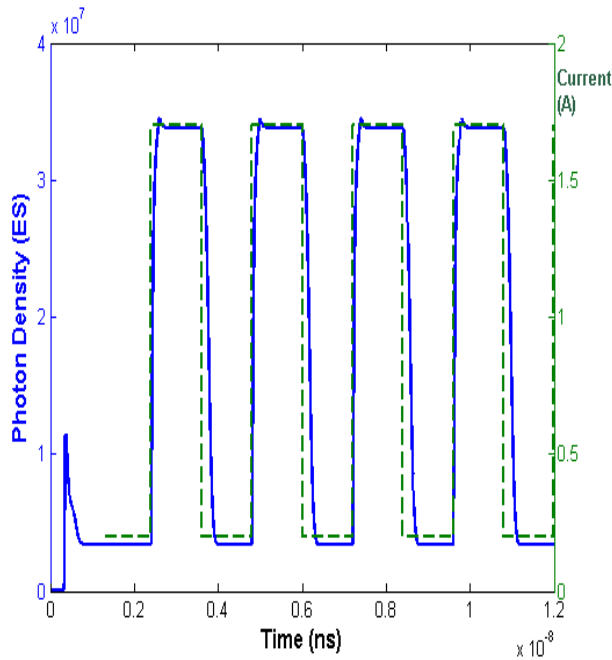

Figure 4: Large signal diagram ofphoton density as a function of time and digital current with presence of compression gain for ES.

In Fig.5 we can clearly see that within ES, when increasing compression gain threshold current for lasing will decrease, unlike GS. As well, output power will decrease when it has become saturated. As such, by comparing the results presented in Fig.5 can turn out to start lasing from higher states we need more bias current since first GS should be saturated and after that with increasing bias current more lasing will start from.

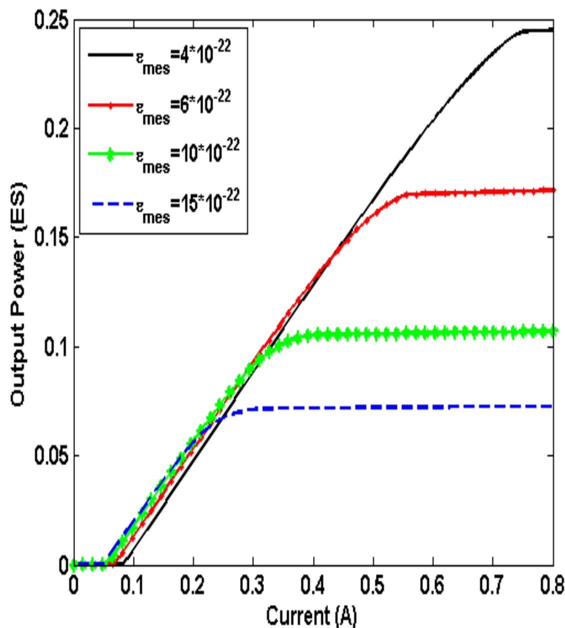

Figure 5: Output power ES as a function of bias current for three values of compression gain.

Table 1 Constant values used in simulations

Parameter	**Value**
Transition energy from GS,E_g	1050 mev
Transition energy from ES, E_e	1090 mev
Transition energy from CS, E_u	1140 mev
Active region length, L_{ca}	1000 μm
Reflectivity of mirrors	R_1=R_2=0.3
Degeneracy of GS, D_g	1
Degeneracy of ES, D_e	3
Degeneracy of CS, D_u	10
Total optical confinement factor, ɼ	0.1
Spontaneous emission coupling factor, β	10^{-7}
Velocity group, V_g	8.571 × 10^7 m/s
Carrier injection rate, η_i	0.9
Spontaneous recombination time, T_{sp}	500 ps
Initial relaxation time from CS to GS, T_{ugo}	2 ps
Initial relaxation time from Es to GS, T_{ego}	6 ps
Initial relaxation time from CS to ES, T_{ueo}	2 ps

Obviously, lasing from ES starts after saturating GS. Similarly, lasing from CS starts after saturating ES. To better understand the effect of compression gain on output power in large modulation for In GaAs/GaAs QD lasers we have calculated output power as a function of time with an AC biased current for ES.

As calculations shown in Fig.6, with increasing compression gain in each state relaxation oscillation reduces with an AC biased current. Next, we will discuss optical gain and its dependence on compression gain for each state separately to determine the optimal values. In Fig.7 optical gain for excited state as a function of bias current is calculated. Clearly, optical gain is not high, and it would be saturated in lower currents when compression gain has increased. At first by increasing bias current from zero, there is a negative optical gain, however by increasing current further, it will become positive, meaning lasing has started efficiently.

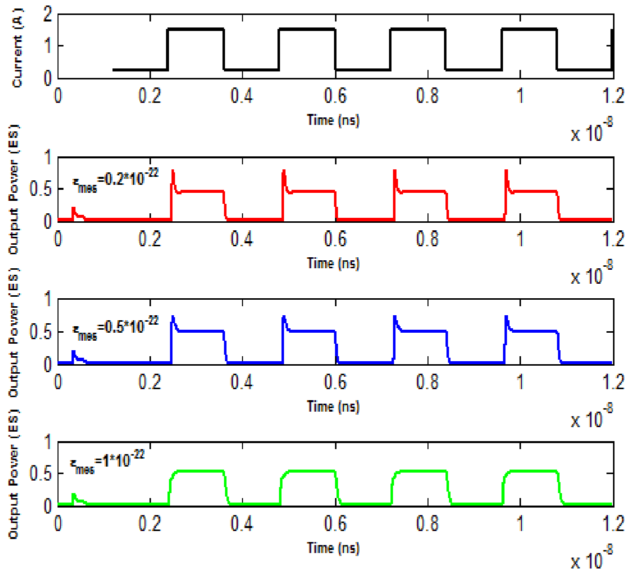

Figure 6: Large signal diagram ofoutput power as a function of time and digital current for three values of compression gain for ES.

To investigate the potential cost effectiveness of this improvement in the area of biomedical imaging we analyzed the small-signal modulation response of this laser design. Fig.8 shows small-signal modulation response for lasing from ES for five values of compression gain. By increasing compression gain frequency response is degraded. Clearly, bandwidth of frequency response in ES is larger than GS. This means that with lasing from ES we will have more bandwidth frequency response, although bias current should be increase too as discussed. Here, if compression gain for ES is $1.5*10^{-22}$ bandwidth of frequency response is about 20 GHz.

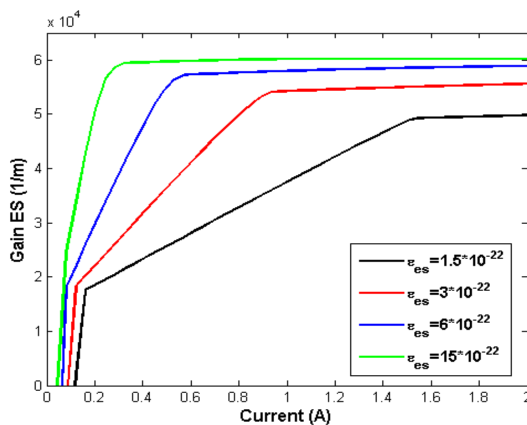

Figure 7: Optical gain for ES as a function of bias current for various compression gain values.

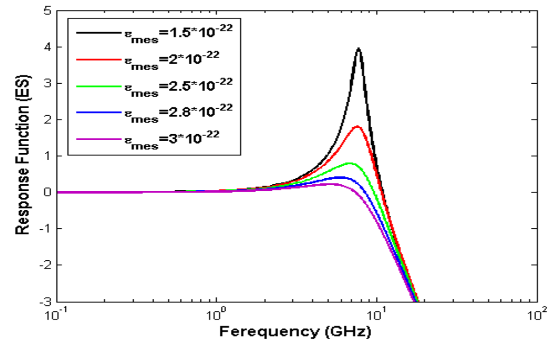

Figure8 : Small-signal modulation bandwidth of In GaAs/GaAs QD laser for ES for some values of compression gain.

IV. CONCLUSION

We have detailed various characteristics for excited states of 1.33 μm self-assembled InGaAs/GaAs QD lasers. We have shown that compression gain is a significant factor in enhancing several crucial properties. A f_{-3dB} modulation bandwidth of GHz was obtained under the DC and AC biasing condition. It can be concluded that with compression gain affects relaxation oscillations in photon density and output power both in DC and AC biased currents(not sure what this sentence is saying). Some f_{-3dB} modulation bandwidth of GHz were obtained for the exited state under the DC biasing condition shown that with reducing compression gain there would be an enhancement in modulation bandwidth of this QD laser that makes it candidate for low cost biomedical imaging purpose.

REFRENCES

[1]. M.V. Maximov, V.M. Ustinov, A.E. Zhukov, N.V. Kryzhanovskaya, A.S Payusov, I.I. NOvikov, N.Y. Gordeev, Y.M. Shernayakov, I. Krestnikov, D. Livshits, S. Mikhrin, A. Kovsh "A 1.33 μm InAs/GaAs quantum dot laser with a 46 cm-1 modal gain", *Sem. Sci. Technol.*, vol**.** **23**, 105004 (2008).

[2]. A. Salhi, G. Raino, L. Fortunato, V. Tasco, L. Martiradonna, M.T. Todaro, M. De Giorgi, R. Cingolani, A. Passaseo, E. Luna, A. Trampert, M. De Vittorio, "Linear increase of the modal gain in 1.3 mu m InAs/GaAs quantum dot lasers containing up to seven-stacked QD layers", *Nanotechnology*, vol. 19, 275401 (2008).

[3]. K. Takada, Y. Tanaka, T. Matsumoto, M. Ekawa, H.Z. Song, Y. Nakata, M. Yamaguchi, K. Nishi, T. Yamamoto, M. Sugawara, Y. Arakawa, "Wide-temperature-range 10.3 Gbit/s operations of 1.3

µm high-density quantum-dot DFB lasers", *Electron. Lett.*, vol. 47, pp. 206-207 (2011).
[4]. F. Lelarge, B. Dagens, J. Renaudier, R. Brenot, A. Accard, F. Van Dijk, D. Make, O. Le Gouezigou, J.G. Provost, F. Poingt, J. Landreau, O. Drisse, E. Derouin, B. Rousseau, F. Pommereau, G.H. Duan, "Recent advances on InAs/InP quantum dash based, semiconductor lasers and optical amplifiers operating at 1.55 µm", IEEE J. Sel. Top. Quant.Electron., vol. 13, pp. 111-124 (2007).
[5]. E. Homeyer, R. Piron, F. Grillot, O. Dehaese, K.Tavernier, E. Mace, J. Even, A. Le Corre, S. Loualiche, "Demonstration of a low threshold current in 1.54 µm InAs/InP(311)B quantum dot laser with reduced quantum dot stacks", Jpn. J. Appl. Phys., vol. 46, pp. 6903-6905 (2007).
[6]. C. Gilfert, V. Ivanov; N. Oehl, M. Yacob, J.P. Reithmaier, "High gain 1.55 µm diode lasers based on InAs quantum dot like active regions", Appl. Phys. Lett., vol. 98, 201102 (2011).
[7]. Shafieenezhad, A., Rajaei, E., & Yazdani, S. (2016). Impact of gain compression on modulation response and dynamic properties of three state lasing InGaAs/GaAs quantum dot lasers. Optics and Spectroscopy, 120(4), 639-645.
[8]. Yazdani, S., Rajaei, E., & Shafieenezhad, A. (2014). Optimizing InAs/InP (113) B quantum dot lasers with considering mutual effects of coverage factor and cavity length on two-state lasing. International Journal of Engineering Research, 3(3), 172-176.
[9]. Shafieenezhad, A., Rajaei, E., & Yazdani, S. (2014). The effect of inhomogeneous broadening on characteristics of three-state lasing InGaAs/GaAs quantum dot lasers. International Journal of Scientific Engineering and Technology, 3(3), 297-301.
[10]. Mikhrin, S.S., Kovsh, A.R., Krestnikov, I.L., et al.: 'High power temperature-insensitive 1.3 µmInAs/InGaAs/GaAs quantum dot lasers', Semicond. Sci. Technol., 20, (5), pp. 340–342 (2005).
[11]. Mi, Z., Bhattacharya, P., Fathpour, S.: 'High-speed 1.3 µm tunnel injection quantum-dot lasers', Appl. Phys. Lett, 86, (15), pp. 153109 (2005).
[12]. Kuntz, M., Fiol, G., Lammlin, M., et al.: '10 Gbit/s data modulation using 1.3 µmInGaAs quantum dot lasers', Electron. Lett, 2005, 41, (5), pp. 244–245.
[13]. Saito, H., Nishi, K., Kamei, A., Sugou, S: 'Low chirp observed in directly modulated quantum dot lasers', IEEE Photon Technol. Lett, 12, (10), pp. 1298–1300 (2000).
[14]. Ghosh, S., Pradhan, S., Bhattacharya, P:'Dynamic characteristics of high-speed In0.4Ga0.6As/GaAs self-organized quantum dot lasers at room temperature', Appl. Phys. Lett., , 81, (16), pp. 3055–3057 (2002).
[15]. N. A. Naderi, M. Pochet, F. Grillot, V. Kovanis, N. B. Terry, and L. F. Lester, "Modeling the injection-locked behavior of a quantum dash semiconductor laser," IEEE J. Sel. Topics Quantum Electron., vol. 15, no. 3, pp. 563–571, May–Jun. (2009).
[16]. P. Bhattacharya, S. Ghosh, S. Pradhan, J. Singh, Z. K. Wu, J. Urayama, K. Kyoungsik, and T. B. Norris, "Carrier dynamics and high-speed modulation properties of tunnel injection InGaAs-GaAs quantum-dot lasers," IEEE J. Quantum Electron. vol. **39**, no. 8, pp. 952–962, Aug. (2003).
[17]. R. R. Alexander, D. T. D. Childs, H. Agarawal, K. M. Groom, H. Y. Liu, M. Hopkinson, R. A. Hogg, M. Ishida, T. Yamamoto, M. Sugawara, Y. Arakawa, T. J. Badcock, R. J. Royce, and D. J. Mowbray, "systematic study of the effects of modulation p doping on 1.3-µm quantum-dot lasers," IEEE J.
[18]. A. Fiore and A. Markus, "Differential gain and gain compression in quantum-dot lasers," IEEE J. Quantum Electron., vol. **43**, no. 3, pp. 287–294, Apr. (2007).
[19]. L. A. Coldren and S. W. Corzine, Diode Lasers and Photonic Integrated Circuits. New York: Wiley, 1995.

Author's details

1. Azam Shafieenezhad, Department of Physics, Indiana University Purdue University Indianapolis, IN, USA, ashafiee@iu.edu
2. Saeed Yazdani, Department of Physics, Indiana University Purdue University Indianapolis, IN, USA, syazdani@iu.edu
3. Esfandiar Rajaei, Department of Physics, University of Guilan, Guilan, Iran, raf404@guilan.ac.ir